JOURNAL OF CATALYSIS 114, 112–120 (1988)

# Thermal Stabilization of Transition Alumina by Structural Coherence with $LnAlO_3$ (Ln = La, Pr, Nd)

FRANÇOIS OUDET, PIERRE COURTINE, AND ALAIN VEJUX

*Département de Génie Chimique, Service d'Analyse Physico-Chimique, Université de Technologie, B.P. 649, 60206 Compiègne Cedex, France*

Received October 7, 1987; revised May 18, 1988

Thermal stabilization of transition alumina is achieved by nucleating a cubic $LnAlO_3$ structure (Ln = La, Pr, Nd) on the surface of the alumina support. The structural transition to corundum is inhibited by strong surface interactions between the thermally stable cubic perovskite compound, $LnAlO_3$, and alumina. A model is proposed to interpret the influence of the doping oxide: the thermal stabilization is related to the presence of $LnAlO_3$ microdomains in the corundum nucleation sites. The strength of the interaction is a result of structural analogies exhibited by the two components of the support ($LnAlO_3$ and $Al_2O_3$), both related to fcc oxygen packings. 

## INTRODUCTION

Thermal stabilization of transition alumina is of primary industrial interest. In particular, the decrease in activity of automotive catalysts, by thermal sintering of the active supported metal components, is dramatically aggravated by modifications around 1000°C of active alumina (*1*). These modifications appear both on structural grounds (transformation of active alumina into corundum) and on textural grounds (loss of specific area and porosity).

Generally, stabilization is obtained by doping the alumina support (and consequently the supported catalyst) with foreign elements such as alkaline-earth metals (*2*), zirconium (*3*), and rare-earth metals (*3, 4*). Among the latter, cerium (*5*) and lanthanum (*3, 6*) are the most commonly used.

In spite of the fact that these systems are extensively studied, the exact nature of the interaction between lanthanum (and related Pr and Nd metals) and alumina is not yet clearly understood.

This paper is an attempt to interpret the thermal stabilization of alumina. A model is proposed, based on structural considerations, with respect to alumina and to a doping phase with the $LnAlO_3$ (Ln = La, Pr, Nd) structure.

## EXPERIMENTAL

*Preparation.* The preparation of these rare-earth-doped aluminas has been described previously (*7*). Briefly, the Ln compounds are deposited on the support by ammonia coprecipitation (pH ≈ 9) of Ln and aluminum hydroxides (both from nitrates) in equimolar mixture (La/Al = 1) in an aqueous suspension of boehmite (Rhône-Poulenc GB200, 200 $m^2/g$). After extensive washing and filtration, the product is calcined at 600°C for 4 h to transform the boehmite into $\gamma$-$Al_2O_3$. Bulk $LnAlO_3$ samples are prepared by similar processes, i.e., thermal decomposition at 800°C of Ln and Al hydroxides, obtained by ammonia coprecipitation of an equimolar mixture of the corresponding nitrates. Finally, Ln oxides are obtained by thermal decomposition of the respective hydroxides. These compounds are used as standards for the UV–visible spectroscopy experiments.

*Surface area determination.* The surface area of the support is measured by the BET method on a Coultronics apparatus.

*X-ray diffraction.* XRD spectra (Cu $K\alpha$,



0021-9517/88 $3.00

$2\theta$) are recorded on a RIGAKU diffractometer, equipped with a proportional counter.

*Transmission electron microscopy.* Selected area diffraction (SAD) and direct imaging are performed on a JEOL JEM 1200 EX microscope, operated at 120 kV.

*UV–visible spectroscopy.* Diffuse reflectance spectra are obtained on a DK-2A Beckman spectrophotometer, in the wavelength range 900–400 nm (transmittance scale).

## RESULTS

We showed in a previous paper (*8*) that the stabilization by lanthanum of alumina is optimum for a cationic ratio of 1% lanthanum (La/La + Al = 0.01); after high-temperature exposure (1150°C), the specific area of the supports is maximum at this concentration. Moreover, for lower La loadings (<1%), alumina partly transforms into corundum. For noble metal exhaust catalysts (*8*), we have established (by hydrogen chemisorption) that the presence of lanthanum increases both the initial metallic dispersion and the resistance to thermal sintering of supported metals. Recently (*9*), we obtained direct confirmation of the thermal stability of lanthanum doped three-way monolithic exhaust catalysts by measuring the evolution of the catalytic activity (conversion of CO, $NO_x$, and hydrocarbons to $CO_2$, $N_2$, and $H_2O$) versus thermal treatments on a laboratory reactivity test (feed-

TABLE 1

Changes in the Surface Area of Ln-Doped and Undoped Alumina after Heating at 600°C, 4 h (a) and 1150°C, 12 h (b)

| Sample | $S_{BET}$ ($m^2/g$) | |
|---|---|---|
| | (a) | (b) |
| Pure $Al_2O_3$ | 250 | 3 |
| 1% La–$Al_2O_3$ | 220 | 63 |
| 1% Pr–$Al_2O_3$ | 220 | 50 |
| 1% Nd–$Al_2O_3$ | 220 | 49 |

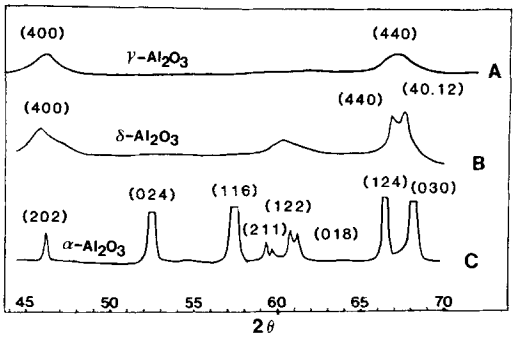


FIG. 1. XRD patterns of La-doped alumina and undoped alumina, before and after thermal aging. (A) Both samples before thermal aging (as prepared). (B) 1% La–$Al_2O_3$ after heating at 1150°C, 12 h. This sample has the $\delta$-$Al_2O_3$ structure. (C) Pure alumina after heating at 1150°C, 12 h. This structure is $\alpha$-$Al_2O_3$.

stream: $NO_x$, CO, $CO_2$, $O_2$, $N_2$, $H_2$, $H_2O$, $C_3H_6$, $C_3H_8$).

In the present paper, we extend to Pr and Nd the study of the stabilization of transition alumina.

Table 1, which gives the BET surface area of pure alumina and of the three 1% Ln-doped samples before and after calcination for 12 h at 1150°C, illustrates the beneficial effect of La, Pr, and Nd on the texture of the alumina support.

The XRD patterns exhibited by the Ln-doped samples are completely identical. Figure 1 shows the changes in the XRD patterns of pure alumina and of 1% La–$Al_2O_3$ (thus representative of the Ln-doped samples) before calcination (as-prepared samples, pattern A), and after thermal aging (1150°C, 12 h).

Comparison of the XRD patterns after heat treatment shows that the doped sample (pattern B) has a transition alumina structure ($\delta$-$Al_2O_3$), whereas the undoped alumina (pattern C) is completely transformed into corundum.

As expected, according to the great similarity of the chemical properties of La, Pr, and Nd, the three rare-earth elements are almost identically effective both on the structure (inhibition of the formation of corundum) and on the texture of the support

(preservation of a high surface area after calcination at 1150°C): 3 $m^2/g$ for pure alumina and, respectively, 63, 50, and 49 $m^2/g$ for La-, Nd-, and Pr-doped supports.

We now attempt to determine the chemical state of the Ln elements responsible for the thermal stability. Given our preparation process, formation of $LnAlO_3$ on alumina support is expected (since bulk $LnAlO_3$ readily forms in such coprecipitation processes followed by calcination above 800°C; see Experimental).

Actually, the XRD patterns (Fig. 1) show that no crystalline phases other than alumina can be detected in the 1% doped samples. Since $LaAlO_3$ peaks are detected for higher concentrations (*8*), we may assume $LnAlO_3$ to be present also with the 1% doped samples, but below the threshold of detection by XRD. The following experiments were aimed at giving more direct confirmation.

TEM experiments have been performed on doped and undoped alumina. While SAD shows the same limitation as XRD in detection of the 1% doping phase, direct imaging (Figs. 2a,b) reveals important differences between the two products, mainly from the point of view of morphology and crystallinity. The doped alumina appears


FIG. 2. Micrographs of the supports after heating at 800°C, 5 h. (a) 1% $La-Al_2O_3$. (b) Undoped alumina [the fringes represent the (111) planes of $\gamma$-alumina, $d$ = 4.56 Å].

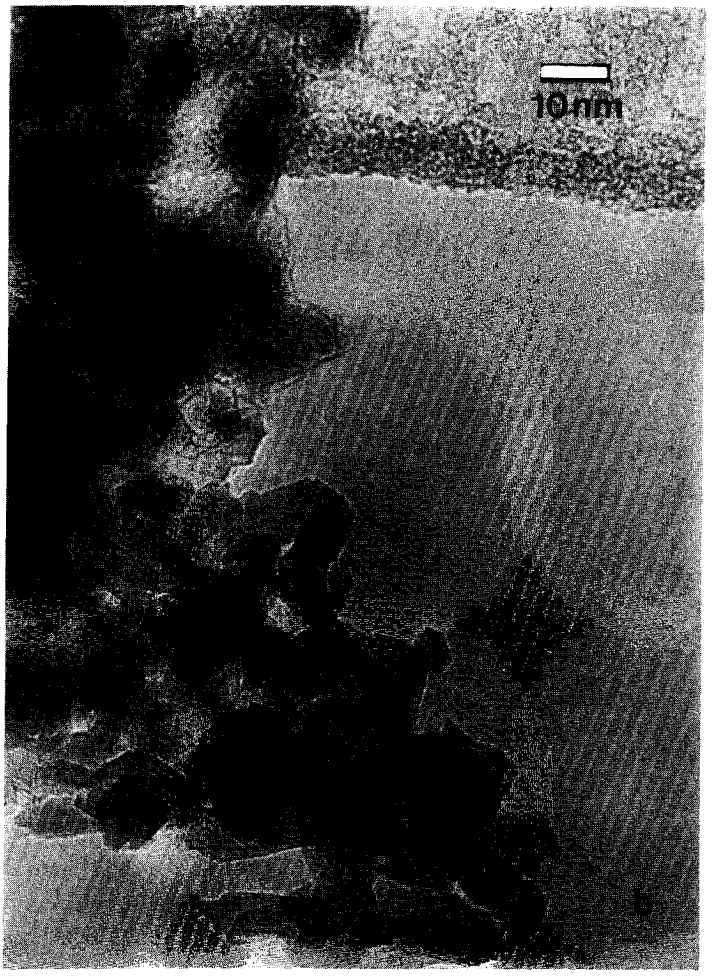


FIG. 2—*Continued.*

less structurally organized and crystallized than pure alumina, even after high-temperature treatments. These differences are discussed in the next section. While confirming the existence of interactions between lanthanum and alumina, this technique does not provide precise information about the chemical state of lanthanum in the doped samples.

Due to the limitations of XRD and TEM methods, more sensitive techniques have to be used. Since UV–visible spectroscopy is known to easily reveal the influence of crystal field on the electronic transitions in *f* orbitals of the rare-earth elements (*10*), the doped samples were characterized by this means.

Figure 3 shows the diffuse reflectance spectra of three neodymium compounds of interest ($Nd_2O_3$, $NdAlO_3$, 1% Nd–$Al_2O_3$). One can see that the three curves are quite comparable. However, the $NdAlO_3$ and 1% Nd-doped alumina spectra, while exhibiting the same energy transition levels, are shifted to the "blue" by approximately 12.5 nm compared with the $Nd_2O_3$ transitions. These results are in good agreement with the data presented by Caro (*10*), concerning the shift of the $^4I_{9/2}$–$^2P_{1/2}$ transition of the $4f^3$ orbital between $Nd^{3+}$ in neodymium ox-

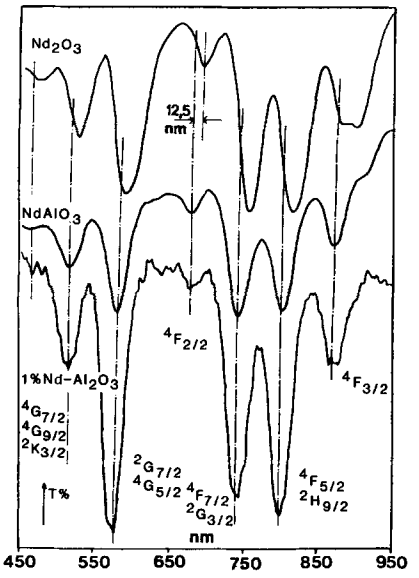


FIG. 3. Diffuse reflectance spectra of $Nd_2O_3$, $NdAlO_3$, and 1% Nd-doped alumina. The similarity of the two last spectra, shifted by approximately 12.5 nm relative to $Nd_2O_3$, indicates the formation of $NdAlO_3$ in the Nd-doped sample. The absorption peaks are attributed to transitions from the $^4I_{9/2}$ level ($4f^3$) to the labeled levels.

ide and the same ion in substitution (of $La^{3+}$) in $LaAlO_3$.

Figure 4 shows the result of the same experiment performed with praseodymium. In this case, the situation is more ambiguous since the praseodymium oxide prepared under the conditions previously described is a nonstoichiometric, deep black powder, and thus does not yield any diffuse reflectance spectrum. However, the spectra of Pr-doped alumina and $PrAlO_3$ are the same, with energy transitions at 600, 495, 475, and 450 nm.

These results indicate the formation of perovskite-type oxides, $PrAlO_3$ or $NdAlO_3$, on the surface of the transition alumina (*11*), since the formation of Ln–$\beta$-$Al_2O_3$ rare-earth aluminate with the $\beta$-$Al_2O_3$ structure is unlikely at the low preparation temperature (*12, 13*). In the case of lanthanum (absence of *f* electrons), this spectroscopic method cannot provide direct evidence for the formation of $LaAlO_3$.

However, the physical and chemical properties of the rare-earth elements are virtually identical (*f* electrons strongly shielded by *s* and *d* electrons), which in our opinion justifies the extrapolation to lanthanum of the results obtained with the two other elements, and the assumption that $LaAlO_3$ forms in La-doped alumina.

## DISCUSSION

### *Morphological Differences between Doped and Pure Alumina at Intermediate Temperatures*

The morphological differences between the doped and undoped alumina (Figs. 2a, b) at intermediate calcination temperature (i.e., before transformation of pure alumina into corundum, and before formation of the $LnAlO_3$ compounds) are now briefly discussed. It is clear from these micrographs that the presence of the doping element on the alumina surface modifies its crystal growth characteristics. Indeed, the doped support appears poorly crystallized, with particles of undefined shape. On the contrary, pure alumina is composed of microcrystals with a geometrical habit, exhibiting the (111) lattice fringes ($d$ = 4.56 Å). We may assume that the presence of the Ln compounds inhibits the development of the

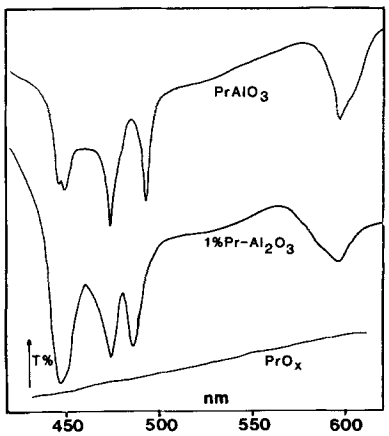


FIG. 4. Diffuse reflectance spectra of $PrO_x$, $PrAlO_3$, and 1% Pr-doped alumina. As in the case of Nd, the similarity of the two last spectra indicates the formation of $PrAlO_3$ in the Pr-doped sample.

surface growing planes of alumina and, consequently, affects the structural and morphological aspects of the support.

The formation of water from surface hydroxyl groups of alumina is directly related to the loss of specific area during the thermal transformation of transition aluminas ($\gamma \rightarrow \delta \rightarrow \theta$) (*3, 14*). This influence of Ln elements on the texture of the supports during the intermediate stages of the thermal treatment ($T < 800$°C) could be related to interactions between $Ln^{3+}$ ions and $OH^-$ groups. As is the case with zeolite compounds (*15*), $La^{3+}$ could undergo a hydrolytic reaction (formation of species such as $La^{3+}$–$OH^-$–$La^{3+}$, by electron withdrawing from the O–H bond), leading to an increase in the acidity of the OH groups. These hydroxyl groups would thus be more difficult to remove from the surface of alumina (*16*). This chemical trapping of OH groups on the surface of the support could explain the morphological differences between doped and undoped alumina at intermediate temperatures.

*Structural Stability of Ln-Doped Alumina*

The experimental results presented in the previous section confirm that the transition alumina structure can be thermally stabilized at high temperature by surface perovskite-type oxides: $LnAlO_3$ (Ln = La, Nd, Pr). The large volume of $O_hLn^{3+}$ ions [$r \approx 1$ Å (*17*)] does not allow one to consider that this stabilization results from the formation of a Ln–$Al_2O_3$ solid solution [i.e., Ln ions in $O_h$ vacancies, or in substitution of $Al^{3+}$ ($r = 0.51$ Å) in the fcc oxygen packing of $\gamma$-alumina] with ions not involved in the $LnAlO_3$ structure. An interpretation of this stabilizing effect must now be proposed.

The fact that the support is shown to be diphasic, composed for the most part of transition alumina and to a lesser extent $LnAlO_3$ compound, leads us to investigate the possibility of interface phenomena located at the phase boundaries between $Al_2O_3$ and $LnAlO_3$.

One can conceive that the low concentration in the rare-earth element makes very difficult the direct observation and characterization of such interfaces. Nevertheless, the structural similitude of both compounds leads us to propose a model based on the possible crystallographic adaptation of the surface lattice planes in the vicinity of the interface.

As demonstrated by Lippens (*18*), the transition $\gamma$-alumina can be considered as derived from the fcc spinel structure. The so-called $\delta$ and $\theta$ forms differ from the $\gamma$ form in their cationic site occupancy; $\delta$-$Al_2O_3$ is a threefold superstructure along the $c$ axis of the $\gamma$ structure (*18*) and $\theta$-$Al_2O_3$, generally indexed in the monoclinic system (by analogy with $\beta$-$Ga_2O_3$), is also closely related to the fcc structure (*19*). According to these remarks, we consider in the following a unified description of the transition alumina structure based on fcc oxygen anion packing ($a = 7.6$ Å), the $Al^{3+}$ cations being distributed as described by Lippens (*18*) and, later by Knözinger and Ratnasamy (*16*) and Gates *et al.* (*20*).

On the other hand, the $LnAlO_3$ (Ln = La, Pr, Nd) structures, while generally indexed in the hexagonal/rhombohedral system (*21*), can be idealized as fcc packings, since they all exhibit a $c/a$ ratio approximately equal to 2.45 (*22*) (respectively, 2.4436, 2.4316, 2.4271). Moreover, according to Wyckoff (*23*), these three cubic aluminates are isomorphous, with lattice parameter $a = 7.6$ Å (the same as for the model spinel alumina).

As previously determined by TEM (8), the $LnAlO_3/Al_2O_3$ interface can be considered as composed of the $(1\bar{1}0)$ planes of both cubic structures.

Figures 5a and b show the proposed model for this interface. Figure 5a represents the projection on the $(1\bar{1}0)$ surface plane of the two structures. Figure 5b is a projection along the $c$ axis of alumina, i.e., perpendicular to the previous direction.

We have previously shown (*24–31*) that when crystallites of two phases belonging

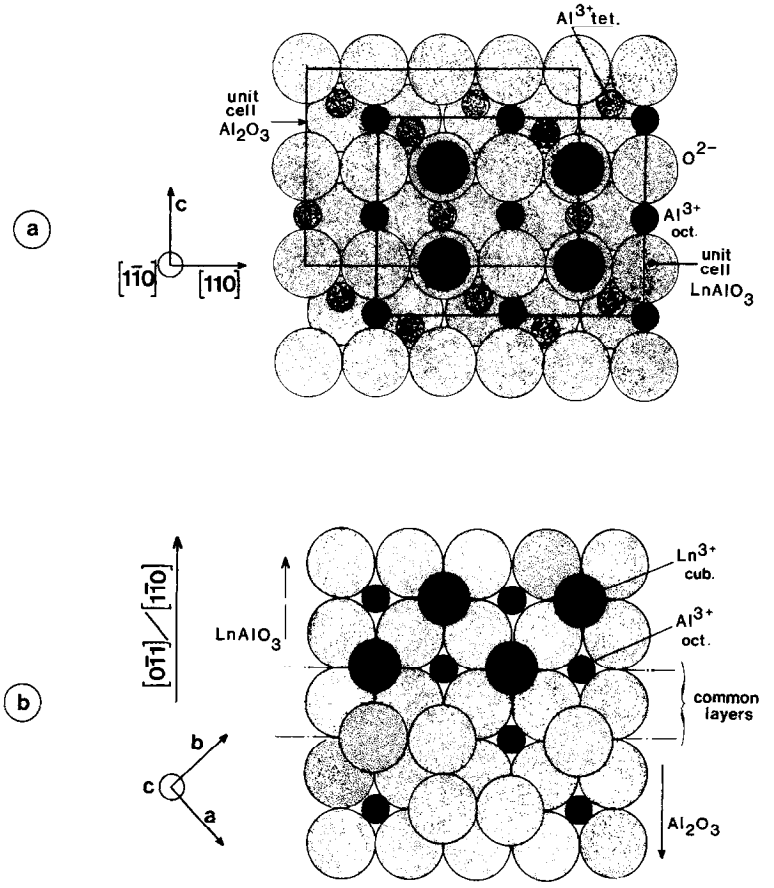


FIG. 5. Model of the $LnAlO_3/Al_2O_3$ interface (both fcc structures). Large circles: $O^{2-}$ ($r$ = 1.32 Å); small circles: $Al^{3+}$ ($r$ = 0.51 Å); large black circles: $Ln^{3+}$ ($r$ = 1 Å). (a) Projection of the (1$\bar{1}$0) interface plane. (b) Projection along the $c$ axis of the alumina unit cell. The coherence of the interface is due to the similarity of the oxygen packing and to the continuity of the $Al^{3+}$ coordination between both structures. The thermal stability of alumina is assumed to be related to the strong interaction resulting from the sharing of two atomic layers between the two unit cells.

to the same parent structures come into contact by some preponderant surface lattice planes exhibiting the same pattern with only a small misfit, coherent interfaces could be formed that could have influence on the catalytic or solid/solid reactivity of the system.

The continuity of the two frameworks is a result of the common nature of both anionic distributions sharing the same lattice parameter and geometric arrangement. The coherence of the interface is also generated by the common coordination of aluminum cations (octahedral) on both sides of the interface. Another contribution to coherence is the respect of the natural cubic coordination of the rare-earth element.

According to this model, the $LnAlO_3/Al_2O_3$ interface can be considered as the connection of two atomic layers between the two structures. One layer belongs to the perovskite structure and does not contain Ln cations, but does contain oxygen and octahedral aluminum ions. The second layer originates from alumina, and all the aluminum cations are octahedral [D-layer as proposed by Lippens (*18*)].

The preceding structural considerations,

showing the possibility of coherent interfaces, are based on a couple of bulk components. The low concentration in rare-earth elements (1%) does not permit complete coverage of the alumina surface by the foreign perovskite oxide. The presence of the doping phase has to be limited to "strategic" areas on the alumina surface. In our opinion, $LnAlO_3$ appears as microdomains, located on the most reactive areas of the alumina surface, i.e., edges and corners of the particles, where the atoms are not fully coordinated, and are, accordingly, unsaturated (strong Lewis acid sites). These areas naturally provide anchoring and nucleation sites for $LnAlO_3$ during the preparation process. Since these reactive areas can also be considered as nucleation sites for the corundum structure [transition alumina transforms into corundum by a nucleation/growth mechanism (*3*)], the effect of the doping compounds can be interpreted as follows:

*The presence in the corundum nucleation sites of the stable perovskite oxide, strongly anchored by means of interfacial coherence, hinders the subsequent surface atomic diffusion and structural rearrangement leading to* $\alpha$-$Al_2O_3$.

Schaper *et al.* (*6*) have previously studied the chemical state of lanthanum in conventionally prepared La-doped alumina (direct impregnation of $\gamma$-$Al_2O_3$ by lanthanum nitrate). By ESR spectroscopy, they showed that lanthanum exhibits the $LaAlO_3$ structure, but did not propose an interpretation of the stabilizing effect of this doping phase. Whereas our preparation process is undoubtedly different from the conventional one, both seem to lead to comparable systems, i.e., composed of transition alumina and of perovskite rare-earth aluminate. Thus, it seems plausible to extend to the conventional preparation processes our interpretation of the stabilizing effect of La, Pr, and Nd on transition alumina.

## CONCLUSION

The present work shows that transition alumina can be thermally stabilized by surface interactions with a perovskite-type oxide, $LnAlO_3$ (Ln = La, Pr, Nd). This thermally stable compound, deposited on the surface of alumina, has a neutralizing effect on the corundum nucleation areas, inhibiting the formation of the stable form of alumina. The strength of the interaction between $LnAlO_3$ and $Al_2O_3$, providing the stability, is believed to be a result of structural analogies exhibited by these two oxides, considered as fcc oxygen packings. Our model proposes an original contribution to the understanding of thermal stabilization of transition alumina. For the sake of completeness, the nucleation process and the exact localization of the doping compounds should be more accurately stated.

Though experimentally based on samples specifically prepared, direct analogy seems to justify the extension of our model to the rare-earth doping effects obtained by conventional preparation processes.

## ACKNOWLEDGMENTS

The authors are very grateful to Dr. J. P. Guerlet and Mr. C. Lambert, both from Comptoir-Lyon-Alemand Louyot, Paris, for financial support. Thanks are extended to Dr. G. Le Flem, Laboratoire de Chimie du Solide, CNRS, Bordeaux, for his very helpful discussion on UV–visible experiments.

## REFERENCES

1. Chu, Y. F., and Ruckenstein, E., *J. Catal.* **55,** 381 (1978).
2. Wyatt, M., Gould, A. M., and Leach, G. M., European Patent 0,056,729 (1982).
3. Burtin, P., Thesis, Ecole Nationale Supérieure des Mines, Saint-Etienne, 1985.
4. Yamashita, H., Kato, A., and Uno, S., European Patent 0,130,835 (1985).
5. Gaugin, R., Graulier, M., and Papée, D., *Adv. Chem. Ser.* **143,** 147 (1975).
6. Schaper, H., Doesburg, E. B. M., and Van Reijen, L. L., *Appl. Catal.* **7,** 211 (1983).
7. Oudet, F., Courtine, P., Lambert, C., Maxant, G., and Guerlet, J. P., French Patent 86,04,267 (1986).
8. Oudet, F., Bordes, E., Courtine, P., Maxant, G., Lambert, C., and Guerlet, J. P., *in* "Studies in Surface Science and Catalysis" (A. Frennet and A. Crucq, Eds.), Vol. 30, p. 313. Elsevier, Amsterdam, 1987.
9. Oudet, F., Thesis, University of Compiègne, 1987.
10. Caro, P., "Structure Electronique des Elements

de Transition." Presses Universitaires de France, Paris, 1976.
11. Le Flem, G., private communication.
12. Dexpert-Ghys, J., Faucher, M., and Caro, P., *J. Solid State Chem.* **19,** 193 (1976).
13. Ropp, R. C., and Carroll, B., *J. Amer. Chem. Soc.* **63,** 417 (1980).
14. Soled, S., *J. Catal.* **81,** 252 (1983).
15. Breck, D. W., "Zeolite Molecular Sieves." Wiley, New York, 1974.
16. Knözinger H., and Ratnasamy, P., *Catal. Rev. Sci. Eng.* **17,** 31 (1978).
17. Shannon, R. D., *Acta Crystallogr. A* **32,** 751 (1976).
18. Lippens, B. C., Thesis, Delft, 1961.
19. Wilson, S. J., *Proc. Brit. Ceram. Soc.* **28,** 281 (1979).
20. Gates, B. C., Katzer, J. R., and Schuit, G. C. A., "Chemistry of Catalytic Processes." McGraw–Hill, New York, 1979.
21. ASTM Files, $LaAlO_3$: No. 9/72, $PrAlO_3$: No. 9/71, $NdAlO_3$: No. 9/73.
22. Guinier, A., "Théorie et Technique de la Radio-Cristallographie." Dunod, Paris, 1956.
23. Wyckoff, R. W., "Crystal Structures," Vol. 2. Interscience, New York, 1964.
24. Courtine, P., *in* "Solid State Chemistry in Catalysis" (R. K. Grasselli and J. M. Bradzil, Eds.), ACS Symp. Ser. Vol. 279, p. 36. Amer. Chem. Soc., Washington, DC, 1985.
25. Jung, J. S., Bordes, E., and Courtine, P., *in* "Adsorption and Catalysis on Oxide Surfaces" (M. Che and G. C. Bond, Eds.), p. 345. Elsevier, Amsterdam, 1985.
26. Papachryssanthou, J., Bordes, E., Courtine, P., Marchand, R., and Tournoux, M., *Catal. Today* **1,** 219 (1987).
27. Véjux, A., and Courtine, P., *J. Solid State Chem.* **23,** 93 (1978).
28. Courtine, P., and Véjux, A., *C.R. Acad. Sci. Ser. C,* 135 (1978).
29. Véjux, A., and Courtine, P., *J. Solid State Chem.* **63,** 179 (1986).
30. Bordes, E., and Courtine, P., *J. Catal.* **57,** 236 (1979).
31. Eon, J. G., and Courtine, P., *C.R. Acad. Sci. Ser. C,* 17 (1979).